J Mater Sci (2012) 47:403–411
DOI 10.1007/s10853-011-5813-0

# Effects of molar substitution of AA pendant on poly(MMA-co-GMA) under UV curing

**Sungchul Hong · Moon-Sun Kim · Byung-Woo Kim**

Received: 25 April 2011 / Accepted: 21 July 2011 / Published online: 4 August 2011

**Abstract** The molar substitution of an acrylic acid (AA) pendant group on a glycidyl methacrylate–methyl methacrylate copolymer was investigated to evaluate its affects on mechanical properties and thermal stability under UV curing. Structural analysis was conducted by Fourier transform infrared spectroscopy and proton nuclear magnetic resonance spectroscopy ($^1$H-NMR) to study the synthetic route of the acrylate copolymer. The mechanical behaviors of AA substituted copolymers were interpreted in terms of both their loss tangent and elongation at the break point, because AA increases the cross-linking density, which is directly proportional to the degree of homopolymerization; this relationship was monitored by $^1$H-NMR with various molar substitutions. In addition, the optical and mechanical properties of the copolymers were also characterized by the extent of AA molar substitution. The optimal behavior was obtained at a molar substitution of 94.3% (equivalent to an AA/GMA molar ratio of 1.4) and satisfied both the transparency (>89.3%) and elongation (>7.4%) requirements for the complex-shaped coatings.

S. Hong · B.-W. Kim (✉)
Department of Chemical Engineering, Sungkyunkwan University, Suwon 440-746, Republic of Korea
e-mail: bwkim@skku.edu

S. Hong
e-mail: Sungchul.hong@gmail.com

M.-S. Kim
Bio/Nano-Fusion Material Research Center, Sungkyunkwan University, Suwon 440-746, Republic of Korea
e-mail: moonsunkim@empal.com

## Introduction

Acrylate materials have been commonly used as surface coating agents, adhesives, bulk resins, and for decorative and protective purposes in industry [1]. Traditionally, to improve the properties (e.g., hardness) of these acrylates, solvent-based curing was used as a finishing process. However, due to stringent environmental regulations, the UV curing method is now widely utilized as an alternative. In addition, this method has many advantages including rapid curing speed, high scratch resistance, and low energy consumption [2].

Glycidyl methacrylate (GMA) is one of the widely used acrylate monomers due to its dual functionality, resulting from the presence of both methacrylic and epoxy groups in the same molecule. Such groups can react with a wide variety of monomers and hence modify the copolymer structure to provide higher durability and flexibility. Consequently, GMA, which has such desirable properties and high chemical resistance, has attracted great interest and is currently contained in a variety of marketed products. For these reasons, many studies have been performed with GMA-based polymers. Methyl methacrylate (MMA) has been found to copolymerize with GMA and the resulting copolymer expressed enhanced properties [3–5]; therefore, poly(MMA-co-GMA) was selected as a model compound for this study.

El-Hamouly et al. [6] synthesized AA branched GMA–MMA copolymers by radical polymerization using non-polar solvents and cross-linking agents to evaluate their cross-linking densities and glass transition temperatures ($T_g$). However, the correlation between the molar substitution of the pendant group and the mechanical properties, important for industrial applications was not investigated. Norakankorn et al. [7] have reported the core/shell structure of glycidyl-functionalized poly(MMA) (PMMA) latex nanoparticles synthesized by microemulsion polymerization. The sequence of the GMA–MMA polymers and their reactivity ratio were also investigated via $^1$H-nuclear magnetic resonance (NMR); however, due to a lack of information, their mechanical properties were not evaluated.

Methyl methacrylate can also form a homopolymer, known as poly(MMA). PMMA exhibits desirable properties including excellent optical qualities, high transparency, low density, relatively high impact strength (although significantly lower than that of polycarbonate and some engineered polymers), good mechanical strength, and an outstanding hydrolytic stability against acid and base hydrolysis. However, it has a low abrasion resistance and a slight amount of friction at low pressure on transparent films can significantly damage its optical quality [1, 8].

In general, there are two methods to overcome the drawbacks of PMMA, which are its low abrasion resistance, comparatively low impact strength, and low thermal stability. One of these methods is to improve the regularity of structural sequence and the other is to substitute the functional pendant group on the backbone. The substitution method is considerably easier than the former due to the restricted synthetic conditions for the highly regular form. In this report, the substitution method was adapted to modify the copolymer backbone with AA groups.

According to Abusafieh et al. [9], the poly(MMA-AA) copolymers, containing both hydrophobic MMA and hydrophilic AA groups have controllable swelling strains, which means their mechanical properties against swelling are very robust. In contrast, have also tried to synthesize poly(MMA-AA) via radical polymerization, that results in a ~2–3% volumetric swelling strain and only ~10–20% loss of modulus and strength overall, suggesting AA is suitable for the proposed application.

The aim of our research is to overcome the drawbacks of the GMA–MMA copolymer, including low abrasion resistance and low thermal stability, and to achieve high flexibility as well as high optical quality [10]. As a result, AA was used as a pendant group to improve the mechanical properties [11] and the effects were evaluated when using various molar substitutions on the backbone [12]. In this report, all of the experiments were carried out under UV-cured conditions. The structure of the copolymer was mainly characterized by NMR and Fourier transform infrared analysis. In addition, a detailed study of the AA effects on the GMA–MMA backbone was conducted using the universal testing machine (UTM). The thermal effect of AA substitution was interpreted by differential scanning calorimetry. Mathematically, the effectiveness of constituent homopolymers in lowering the glass transition temperature of a polymeric composition is directly proportional to its glass transition temperature [13, 14] and to its weight fraction ($W$) in the total composition, which are expressed in the inverse weighted average rule as,

$$(1/T_g) = (W_1/T_{g1}) + (W_2/T_{g2}) \tag{1}$$

where $W_1$ and $W_2$ are the weight fractions of the copolymer constituents, and $T_{g1}$ and $T_{g2}$ are the constituent homopolymers glass transition temperatures, respectively [9, 15].

This study was conducted to evaluate the mechanical properties of the polymers with a decorative and protective thin layer applied onto the substrate surface. The thin layer consisted of a complex-shaped component, which exhibits reasonable flexibility and hardness for protective purposes.

## Experimental

### Materials

GMA obtained from Junsei Chemical, Tokyo, Japan with 98% purity was used for copolymerization. MMA at 99% purity was purchased from Dae Jung Chemical, Shiheung, Korea. AA at 99% purity was provided by Dae Jung Chemical, Korea, and used as a monomer to improve mechanical properties. The solvent butyl acetate (BAc) was supplied by Dae Jung Chemical, Korea. 1-dodecylmercaptan (DM), used for chain transfer, was obtained from ACROS, Geel, Belgium. The radical initiator 2,2-azobisisobutyronitrile (AIBN), and the catalyst triphenylphosphine ($PPh_3$) were purchased from Dae Jung Chemical, Korea. 4-methoxyphenol (MPh) provided by Junsei Chemical, Japan, was used as an inhibitor prior to UV curing. Irgacure 184 (HCPK), used as a radical photoinitiator, was obtained from Ciba-Geigy Co., Italy, and the hardener, Coronate HXR was provided by Nippon Polyurethane Industry, Japan. Substrate polyethylene terephthalate (PET) film at 23 μm (model: SM30, transparency 92%) was supplied by SKC Co., Korea. These reagents were used as received without further treatment.

### Synthesis of GMA–MMA copolymers

Earlier studies [6, 7, 9] have reported various methods to synthesize the GMA–MMA copolymer. One of the convenient and simple methods is the use of free radicals, and this process is also utilized commercially. In this article, this method is also employed to achieve both the flexibility and the hardness of the copolymers by controlling the substitution of the AA pendant group.

GMA–MMA was obtained from solution radical polymerization. First, an excess amount of solvent (100 g of BAc, 0.86 mol) was introduced into the reactor, followed by the addition of GMA (17.5 g, 0.12 mol), MMA (7.5 g, 0.07 mol), AIBN (7.5 g, 4.56 × $10^{-3}$ mol), and dodecylmercaptan (0.13 g, 6.42 × $10^{-4}$ mol), which were then stirred at 90 °C for 2 h. Then, GMA (52.5 g, 0.36 mol), MMA (22.5 g, 0.22 mol), AIBN (2.25 g, 0.01 mol), and dodecylmercaptan (0.37 g, 1.82 × $10^{-3}$ mol) were added drop-wise and the reaction mixture was stirred at 90 °C for 5 h followed by a further addition of AIBN (1 g, 6.08 × $10^{-3}$ mol). The mixture was then stirred at 90 °C for 1 h and subsequently heated to 120 °C for 2 h before cooling to 60 °C. Table 1 shows the degree of conversion during polymerization optimization and the reason why two monomer additions were performed. These procedures formed the backbone (GMA–MMA) of the acrylate copolymer with a high degree of conversion. Unless otherwise mentioned, all experiments were performed under a nitrogen atmosphere. For the AA branched copolymer, AA (50.4 g, 0.7 mol) was introduced into the GMA-MMA mixture, along with methoxyphenol (0.14 g, 1.12 × $10^{-3}$ mol) and triphenylphosphine (0.54 g, 2.05 × $10^{-3}$ mol). These components were stirred at 110 °C for 8 h, during which air was bubbled into the solution. To complete the reaction, methoxyphenol (0.14 g, 1.12 × $10^{-3}$ mol) was added to the GMA–MMA acrylate copolymer with pendant AA. The structural details of the backbone and the type of the copolymer were confirmed by Fourier transform infrared spectroscopy (FTIR) (Fig. 2), and the reaction mechanism is described in Fig. 1.

### Preparation of specimens

Different amounts of photoinitiator (Irgcure) and hardener (Coronate HXR) were mixed into solution, and the acrylate copolymer containing the photoinitiator and hardener was deposited onto a PET film using a lab coater (KPM-300, Kee-Pae Trading Co., Korea) and a coating bar (Webster Co., U.S.A, #6). The coating speed was 5–100 mm $s^{-1}$ and the quantity of application was 0.6–4.6 g $m^{-2}$. After irradiation at 700 mJ $cm^{-2}$ (wavelength: 365 nm), a film of 3–5 μm in thickness was obtained. Moreover, the molded dog bone shaped specimen was prepared to investigate the mechanical properties via UTM.

### Analytical measurements

Structural analysis of the backbone and the final copolymer with pendant AA was conducted using a FTIR spectrophotometer (Bruker IFS-6/S, Germany). The spectrum recorded the conversion of double bonds and also exhibited the peaks for different functional groups. The chemical structures and the molar ratios of specific molecules were analyzed by NMR (Unit Inova 500NB, Varian, Santa Clara, U.S.A), using $CDCl_3$ as the solvent for $^1$H-NMR. In addition, the $M_w$ of the copolymer and its distribution were estimated by gel permeation chromatography (GPC, 1100S, Agilent, Santa Clara, U.S.A). This measurement was carried out at room temperature with THF as an eluent at a flow rate of 1 mL $min^{-1}$ using a refractive index detector. The flexibility of the coated film was estimated using a cylindrical bending test device according to the standard test methods (ASTM) for the Mandrel bend test of attached organic coatings D522. The transmittance was measured using an optical hazemeter (SEP-H, Nikon Seimitsu Kogaku, Japan), where the haze increases with the increase of cross-linking density due to the AA substitution. The mechanical properties were obtained by the universal testing machine (UTM, 5565, Instron Co., Grove, U.S.A). A dynamic mechanical analyzer (DMA, SS610, Seiko Exstar, Japan) was used to determine the thermogram of the copolymer which was scanned from 25 to 350 °C at a heating rate of 5 °C $min^{-1}$ at 1 Hz.

## Results and discussion

### Structure of the acrylate copolymer

All experiments were performed after photopolymerization (700 mJ $cm^{-2}$, 365 nm) because each sample should be tested as a final product, and photopolymerization characterizes the non-free monomer in the specimens.

These reaction schemes are shown in Fig. 1, and the structural details were confirmed by $^1$H-NMR (Fig. 3). In Fig. 1, the final form shows the secondary alcohol, and the

**Table 1** Degree of conversion with different addition steps

| No. | Step 1 (first addition) | Step 2 (second addition) | | | | DC (%) |
|---|---|---|---|---|---|---|
| | 2 h | 2 h | 3 h | 1 h | 2 h | |
| C1 | S | | n-S | | | 90 |
| C2 | n-S | S | | n-S | | 67 |
| C3 | S | S | | n-S | | 88 |
| C4 | S | S | | S | n-S | 83 |
| C5 | S | S | n-S | n-S | | 88 |

*S* addition sequence of monomer and constituents with solvent in radical polymerization for GMA–MMA, *n-S* addition sequence of monomer and constituents without solvent in radical polymerization for GMA–MMA

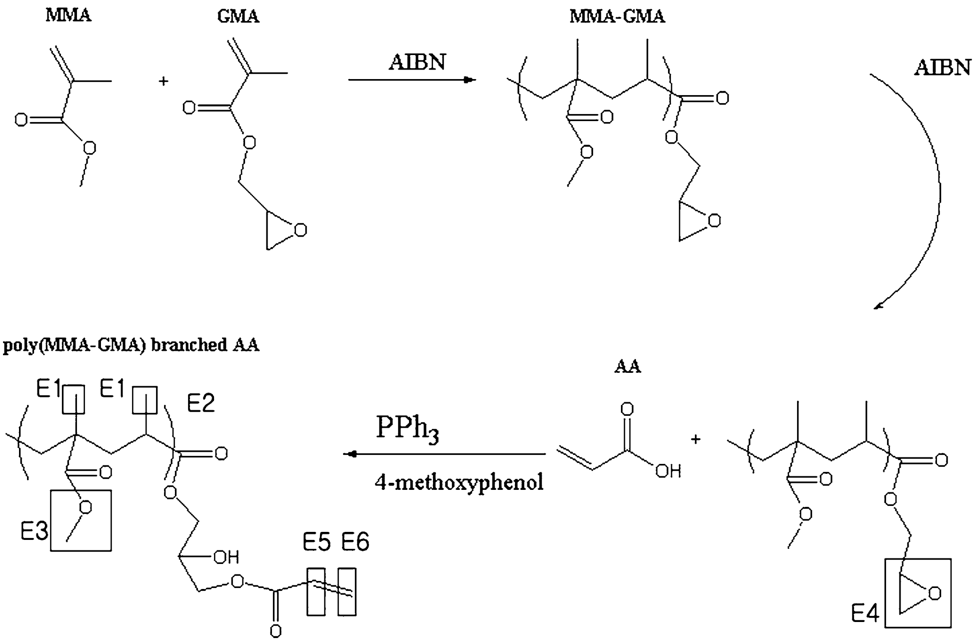

**Fig. 1** Reaction mechanism used to synthesize the GMA–MMA copolymer with AA pendant

AA connected to the primary carbon due to the secondary alcohol are more stable than the primary alcohol [16–18].

The FTIR spectra in Fig. 2 provide information concerning the acrylate structure. The peaks around 810 and 990 $cm^{-1}$ were ascribed to the weak symmetric stretch band of the epoxide in the backbone (Fig. 2a).The disappearance of these two peaks in Fig. 2b indicates that the epoxide ring was opened to branch to the pendant group (AA). In general, the carbonyl group strongly absorbs in the range of 1850–1650 $cm^{-1}$ due to its large change in dipole moment. Because the carbonyl stretching frequency was very sensitive to the attached atoms, it was very easy to detect. The peak at 1737 $cm^{-1}$ was due to the C=O stretching vibration of MMA and GMA ester groups present in the backbone. C=O stretch appears in the range of 1750–1735 $cm^{-1}$ for most of the aliphatic esters.

The FTIR spectrum of the acrylate copolymer showed a band around 3050 $cm^{-1}$ corresponding to the C–H stretching, which is shown in Fig. 2b. The peak at 2960 $cm^{-1}$ was ascribed to C–H asymmetric stretching of a methyl group ($-CH_3$) in Fig. 2a and b. Non-conjugated C=C medium stretching at 1640 $cm^{-1}$ and the strong out-of-plane deformation of C=C at 970 $cm^{-1}$ corresponded to the vinyl group peaks of AA. The medium broad O–H stretching band was also observed at 3500 $cm^{-1}$ (Fig. 2b) and such a peak did not exist in the non-pendant backbone (Fig. 2a) because the epoxide (Fig. 2b) was opened to the secondary alcohol and the primary carbon connected to the AA.

The α-methyl proton ($-CH_3$) originated from PMMA and poly(glycidyl methacrylate) (PGMA) appeared at 0.9 and 0.98 ppm, respectively. For the random copolymer, these peaks were only 0.08 ppm apart and almost overlapped with the PMMA peaks, indicating the random copolymerization of backbone suggested by Norakankorn et al. [7] and Ergozhin et al. [19]. In addition, according to the *Q*–*e* scheme of Alfrey and Prince, the reactivity ratios of the monomers are $r_{GMA} = 1.28$ and $r_{MMA} = 0.75$, and the calculated Q–e values are $Q_{GMA} = 0.96$, $Q_{MMA} = 0.78$, $e_{GMA} = 0.2$, and $e_{MMA} = 0.4$ [7]. This suggests GMA would easily react with GMA or MMA incorporated polymer chains. However, in this correlation procedure, because the product of the reactivity ratios is $r_{GMA}r_{MMA} = 0.96$ and very close to a value of 1, the resulting copolymerization of MMA and GMA occurred in random manner. In Fig. 4c, the peaks around 1.6 and 2.1 ppm corresponded to the backbone (E2) with

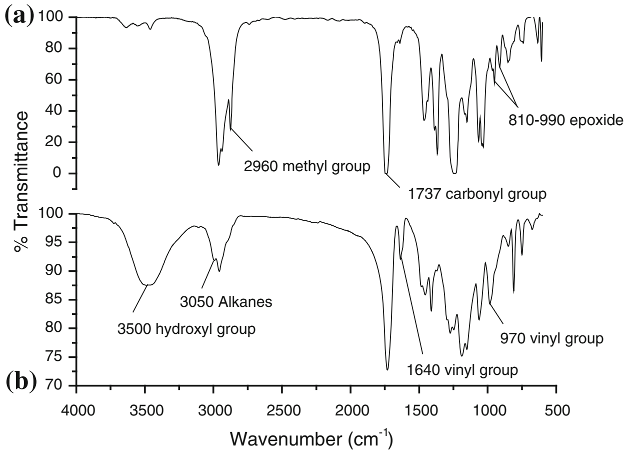

**Fig. 2** FTIR spectra of (**a**) backbone (GMA–MMA) (**b**) backbone with AA pendant

α-methyl groups (E1). The peak at 3.6 ppm (E3) was ascribed to the methoxy group of the MMA. As shown in Fig. 3b the epoxide proton peak originated from GMA and initially appeared at 2.6–3.3 ppm (E4), but then dramatically reduced in height and re-appeared at around 6.5 ppm (E5) and 5.9–6.2 ppm (E6) due to the opening of the epoxide. Overall, these peak shifts are useful features for characterizing the AA molar substitution (Fig. 8). Furthermore, MMA has its own ester group that prevents it from reacting with AA, which contains the ester group. Thus, GMA was used as a coupling agent to form an acrylate copolymer via epoxide opening. The subsequent spectrum is shown in Figs. 1 and 4, where the vinyl group is attached as a branch of the copolymer. Therefore, both FTIR and $^1$H-NMR spectra proved that GMA–MMA copolymer was successfully branched with the AA pendant.

## Thermal and mechanical properties

The amount of each component, such as the co-monomers of MMA, GMA, DM, AIBN, and many others, for the acrylate copolymer are listed in Table 2.

Table 2 shows the effect of the GMA/MMA molar ratio on the $M_w$ during polymerization. For the case where the two monomer (GMA and MMA) reactivity ratios were different, that is, $r_{GMA} > 1$ (=1.28) and $r_{MMA} < 1$ (=0.75), GMA was more reactive than MMA toward both propagating species, and the $M_w$ increased considerably once the GMA/MMA ratio exceeded 1.6. The flexibility of the copolymers relied on both the $T_g$ and the $M_w$. Figures 4, 5, 6 indicate the dynamic mechanical behavior when varying GMA/MMA molar ratio, as described in Table 2.

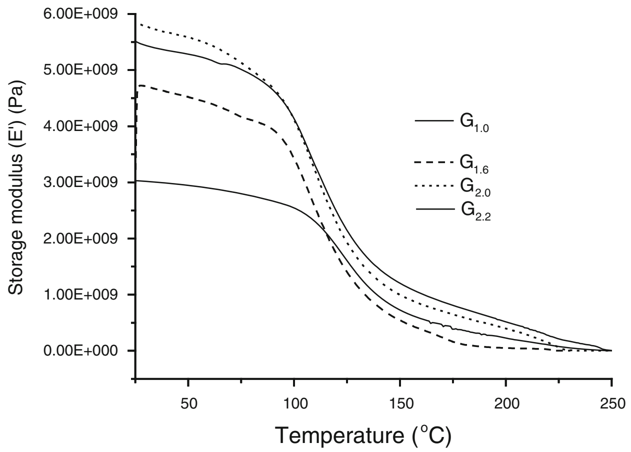

**Fig. 4** Effect of temperature on the storage modulus of GMA-based acrylate copolymer with AA pendant as a function of the molar ratio (GMA/MMA) at a frequency of 1 Hz

The specimens were prepared as a photo-polymerized thin layer on the PET (25 μm, 54,830 KN m$^{-2}$) film,

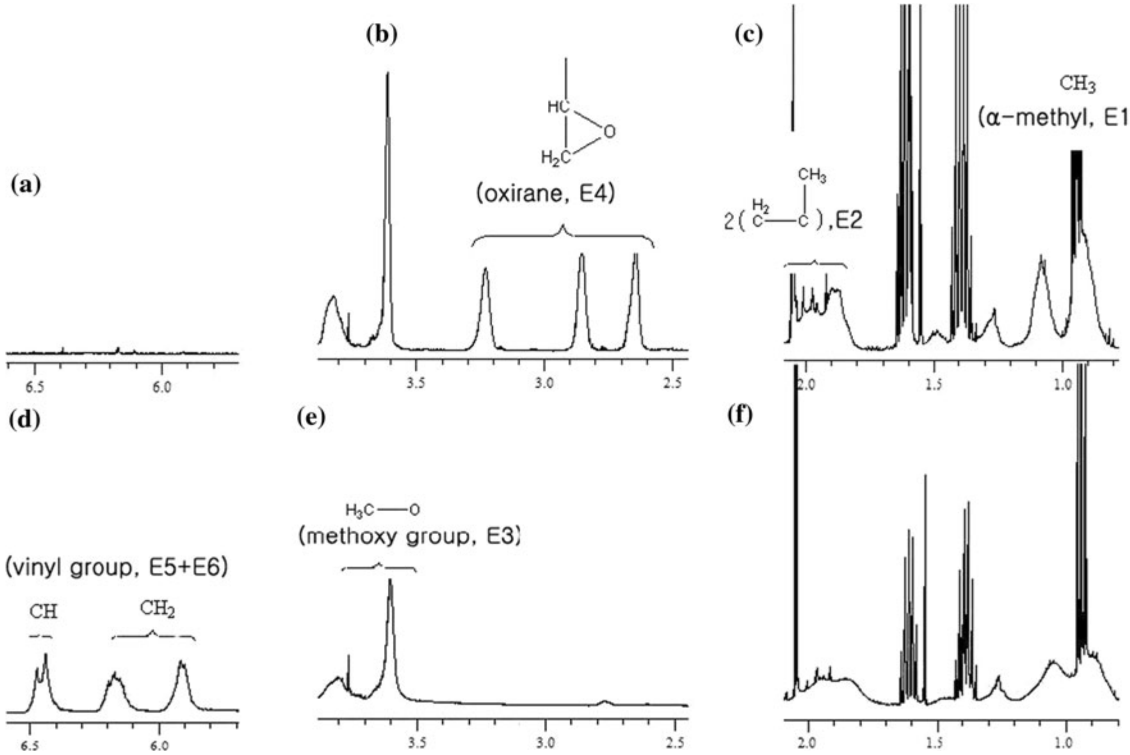

**Fig. 3** $^1$H-NMR spectra of backbone without pendant (from **a** to **c**) and the acrylate copolymer with pendant (from **d** to **f**, E1–E6 were from Fig. 2)

**Table 2** Amount of constituent with a varying molar ratio of GMA/MMA

| No. | Molar ratio of GMA/MMA | MMA (g) | GMA (g) | AA (g) | DM (g) | AIBN (g) | BAc (g) | MPh (g) | $PPh_3$ (g) | HCPK (g) | HXR (g) | $M_w$ |
|---|---|---|---|---|---|---|---|---|---|---|---|---|
| $G_{1.0}$ | 1.0 | 30.0 | 42.7 | 21.6 | 0.5 | 4.0 | 100 | 0.2 | 0.54 | 0.5 | 1.0 | 20,800 |
| $G_{1.6}$ | 1.6 | 30.0 | 70.0 | 36.0 | 0.5 | 4.0 | 100 | 0.2 | 0.54 | 0.5 | 1.0 | 21,200 |
| $G_{2.0}$ | 2.0 | 30.0 | 84.0 | 43.2 | 0.5 | 4.0 | 100 | 0.2 | 0.54 | 0.5 | 1.0 | 34,080 |
| $G_{2.2}$ | 2.2 | 30.0 | 93.1 | 46.8 | 0.5 | 4.0 | 100 | 0.2 | 0.54 | 0.5 | 1.0 | 51,400 |

which was used as the reference for DMA analysis. The viscoelastic polymer was studied by DMA (tension mode, 50 mN, 1 Hz), where a stress is applied to a material and the resulting strain is measured. A perfectly elastic solid and a purely viscous fluid have characteristics where some phase lag (from a 90° phase to in phase) will occur during DMA tests.

Both the intermolecular and intramolecular interactions greatly influence the dynamic storage modulus, which varies with the different physical states of a polymer system [20]. In Fig. 4, $G_{1.6}$–$G_{2.2}$ ($G_{1.0}$–$G_{2.2}$ were shown in Table 2 as sample numbers) exhibited single transitions, indicating the presence of a homogeneous phase that was neither PGMA nor PMMA. At a lower temperature, below $T_g$, $G_{1.0}$ expressed a relatively lower modulus than the others ($G_{1.6}$–$G_{2.2}$) due to the smaller amount of AA pendant with oxirane in the GMA. As a consequence, fewer pendants would lead to a lower cross-linking density and lower entanglement. In addition, $G_{1.0}$ showed a broad transition after the glassy region in a low storage modulus, which suggested the rare appearance of a heterogeneous state.

The effect of molar ratio (GMA/MMA) on the loss modulus in $G_{1.0}$–$G_{2.2}$ was investigated. The observation of single glass transition peaks suggested the presence of a homogeneous phase as shown in Fig. 5. However, these peaks cannot be used to predict the glass transition temperatures that are determined solely by the loss tangent (Fig. 6). When representing the elastic portion, the storage modulus measures the stored energy, and when representing the viscous portion, the loss modulus measures the energy converted to heat. Therefore, both the loss modulus and the storage modulus are analyzed before measuring the loss tangent ($T_g$), which represents the angle between the in-phase and out-of-phase components in the cyclic motion. The loss modulus of $G_{1.0}$ displayed the highest glass transition region, which means that the lower mole fraction of GMA produced a less flexible copolymer. Therefore, the adequately low fraction of GMA should be attributed to the AA pendant attachment instead of a homopolymer formation. In general, the molecular interactions of a simply structured polymer (less branched or linear) are likely to affect the molecular motion. Particularly, they can lead to a higher loss modulus, considering there would be only a small energy barrier to overcome.

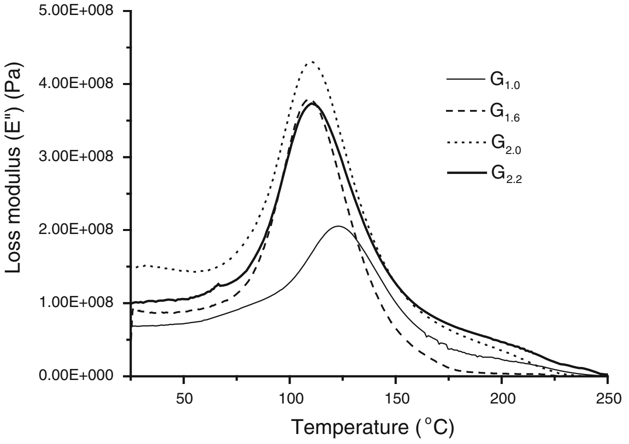

**Fig. 5** Effect of temperature on the loss modulus of GMA-based acrylate copolymer with AA pendant as a function of the molar ratio (GMA/MMA) at a frequency of 1 Hz

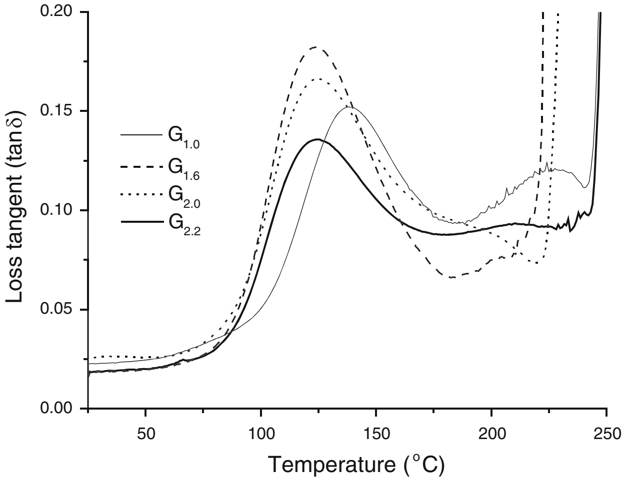

**Fig. 6** Effect of temperature on the loss tangent (tan $\delta$) of GMA-based acrylate copolymer with AA pendant as a function of the molar ratio (GMA/MMA) at a frequency of 1 Hz

The peaks at 121.5, 122.3, and 119.9 °C corresponded to the glass transition temperatures of $G_{1.6}$, $G_{2.0}$, and $G_{2.2}$, respectively. $G_{1.0}$ exhibited the highest peak at 136.8 °C, which indicated the highest thermal stability and rigidity, despite a relatively low loss tangent. However, the highest glass transition temperature of $G_{1.0}$ corresponded to a decrease in flexibility, where the coatings cannot be applied onto a curved part. Therefore, $G_{1.6}$ was chosen as the optimal GMA/MMA ratio for the backbone synthesis, because $G_{1.6}$ exhibited the highest loss tangent, which means that the backbone had both reasonable flexibility and thermal stability, due to the relatively low mole fraction of GMA. Overall, it is important to have a minimum amount of GMA, which has its own $T_g$ as low as 63 °C, to prevent a decrease of thermal stability.

From the results in Figs. 4, 5, 6; Table 3 summarizes the compositions at a fixed GMA/MMA molar ratio of 1.6, while varying the molar ratio of AA/GMA. These contrasting results are due to the different polymerization mechanisms in which the GMA–MMA copolymer was formed via solution radical polymerization. While the pendant AA-forming procedure was performed using radical polymerization with an inhibitor, this resulted in an unreacted monomer. AA has the lowest molecular weight among the monomers used, so the comparatively higher concentration of AA prevented the formation of a higher $M_w$ copolymer and encouraged the formation of lower $M_w$ pendant groups. Nevertheless, PAA (theoretical $T_g$ of 130 °C) has a $T_g$ value higher than those of PGMA (theoretical $T_g$ of 63 °C) and PMMA (theoretical $T_g$ of 115 °C), and thus induced an increase in the $T_g$ of the copolymer (Fig. 7).

The glass transition temperatures of $A_{1.0}$, $A_{1.4}$, and $A_{2.0}$ were 134.8, 136.0, and 137.5 °C, respectively. In the case of $A_{2.0}$, the loss modulus was significantly low for the storage modulus, which is related to the lowest loss tangent. This value of $A_{2.0}$ is also the most comparable to the elastomer. The lowest glass transition temperature was exhibited by $A_{0.6}$ at 131.8 °C due to the highest loss modulus, when compared with the corresponding storage modulus at the same temperature. Figure 7 shows the greatest thermal stability was demonstrated by increasing the molar ratio of AA/GMA. However, the optimal conditions of interest require a perfect balance among flexibility, hardness, and transparency. There are commercial standards desired for complex-shaped coatings. The elongation (representing flexibility), hardness (representing protective layer) and transparency (degree of clearness) should be >7%, over 1H (for insert film) and 85%, respectively. Therefore, $^1$H-NMR was employed to study the relationship between the transparency and the molar substitution of the pendant group.

To determine the molar substitution, the intensities of the vinyl groups of acrylic acid peaks at around 5.9 and 7.0 ppm (E5 + E6) were measured against the intensities of the oxirane ring (E4) peaks at 2.6–3.3 ppm (Fig. 8).

The molar substitutions of $A_{1.0}$, $A_{1.4}$, and $A_{2.0}$ were 93.5, 94.3, and 94.8%, respectively, whereas that of $A_{0.6}$ was <85%. These results indicated that a higher AA/GMA molar ratio > 1.0) did not increase the level of AA pendant branching in the copolymer. Instead of bonding the oxirane, the excess amount of AA self cross-linked and hence homopolymerized.

A similar molar substitution in the range of 93.5–94.8% was assigned to $A_{1.0}$–$A_{2.0}$, suggesting the existence of an AA pendant on the opened oxirane at an AA/GMA molar > 1.0. In spite of the similar molar substitution, the transparency was considerably different (Fig. 9). It was sharply decreased by the increased level of AA

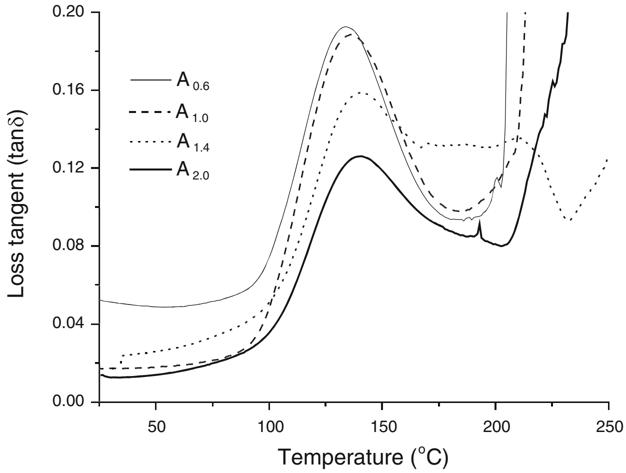

**Fig. 7** Effect of temperature on the loss tangent of GMA-based acrylate copolymer with AA pendant as a function of the molar ratio (AA/GMA) at a frequency of 1 Hz

**Table 3** Composition of constituent with a varying molar ratio of AA/GMA

| No. | Molar ratio of AA/GMA | MMA (g) | GMA (g) | AA (g) | DM (g) | AIBN (g) | BAc (g) | MPh (g) | $PPh_3$ (g) | HCPK (g) | HXR (g) | $M_w$ |
|---|---|---|---|---|---|---|---|---|---|---|---|---|
| $A_{0.6}$ | 0.6 | 30.0 | 70.0 | 21.6 | 0.5 | 4.0 | 100 | 0.2 | 0.54 | 0.5 | 1.0 | 23,200 |
| $A_{1.0}$ | 1.0 | 30.0 | 70.0 | 36.0 | 0.5 | 4.0 | 100 | 0.2 | 0.54 | 0.5 | 1.0 | 21,500 |
| $A_{1.4}$ | 1.4 | 30.0 | 70.0 | 50.4 | 0.5 | 4.0 | 100 | 0.2 | 0.54 | 0.5 | 1.0 | 13,300 |
| $A_{2.0}$ | 2.0 | 30.0 | 70.0 | 72.0 | 0.5 | 4.0 | 100 | 0.2 | 0.54 | 0.5 | 1.0 | 12,900 |

**Fig. 8** Determination of the molar substitution of AA pendant by $^1$H-NMR (**a** $A_{0.6}$, **b** $A_{1.0}$, **c** $A_{1.4}$, **d** $A_{2.0}$, E4–E6 were from Fig. 2)

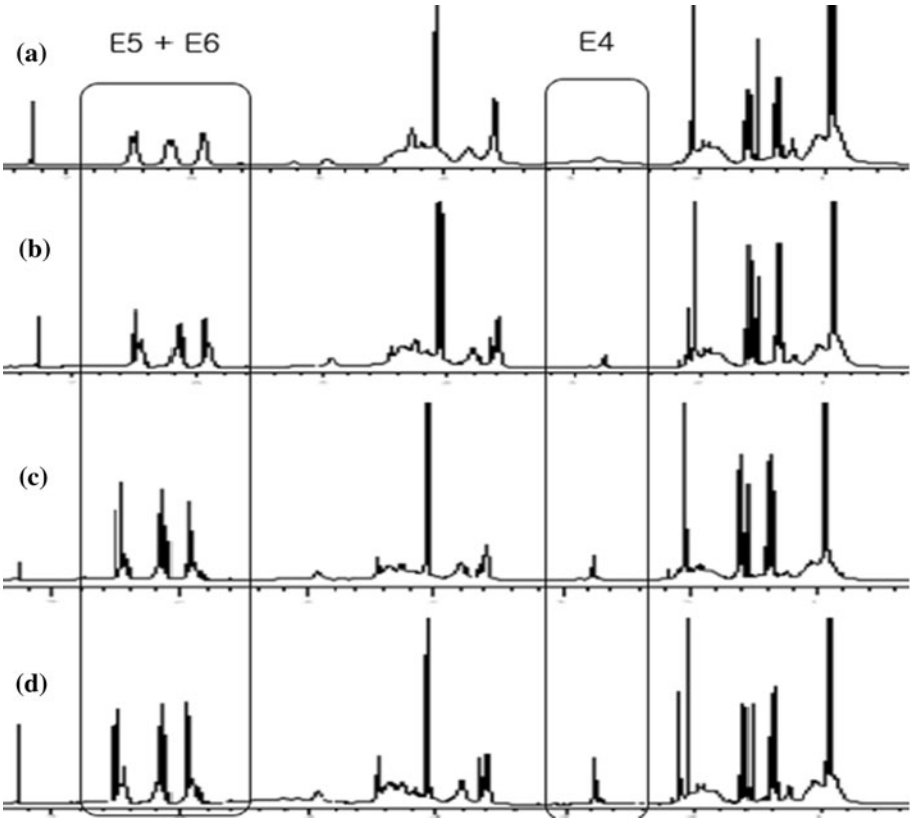

homopolymerization, which causes the cross-linking density to increase. Moreover, as suggested in Table 4, molar substitution is expected to affect the mechanical properties. The elongation at break point and the tensile strength, when varying molar substitution, were measured by UTM and the Mandrel bend tester.

All experiments conducted under these conditions achieved a hardness > 1H, which means that the terms desired for insert film layer were satisfied.

As shown in Fig. 9, the tensile strength was significantly increased from $A_{1.0}$ above (in Table 4). The elongation and the tensile strength were directly proportional to the AA molar substitution because AA is an excellent cross-linking agent and able to homopolymerize. However, the tensile strength increased comparatively slowly at an AA/GMA molar ratio of 1.0, which was the opposite of the transparency.

The results obtained for the mechanical properties were inversely consistent with both Figs. 8 and 9, where the optimal condition was achieved in $A_{1.4}$, which is ascribed to an AA pendant molar substitution of 94.3%, or equivalently, an AA/GMA molar ratio of 1.4. Overall, $A_{1.0}$ was expected to be the best solution, but with a lower elongation than $A_{1.4}$. Regardless, the elongation must satisfy the 7.4% standard for complex-shaped coatings.

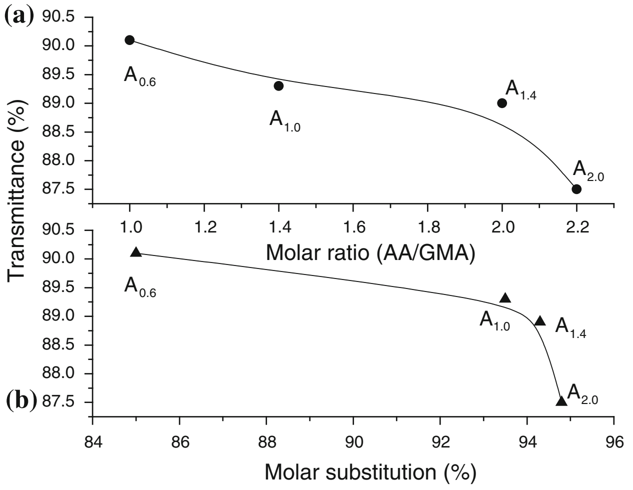

**Fig. 9** Effect of **a** the molar ratio of AA/GMA and **b** the molar substitution on transparency of the coated PET film

## Conclusions

The FTIR and $^1$H-NMR spectra provided information on the structures and mechanisms of acrylate copolymerization with an AA pendant. The AA pendant group was bound to the opened oxirane rings in the GMA backbone. These bindings were observed in the $^1$H-NMR spectrum with methylene and methane at 5.9–6.5 ppm, and in the FTIR peaks at 850–910 cm$^{-1}$.

**Table 4** Mechanical properties of acrylate copolymer with a varying molar substitution of AA

| Sample no. | Elongation (ε), ASTM D522 | Tensile strength (N $m^{-2}$) | Reference (PET, 25 µm, KN $m^{-2}$) |
|---|---|---|---|
| $A_{0.6}$ | $\varepsilon < 7.4\%$ | 111 | 54,830 |
| $A_{1.0}$ | $\varepsilon < 7.4\%$ | 519 | |
| $A_{1.4}$ | $7.4\% < \varepsilon < 14.5\%$ | 602 | |
| $A_{2.0}$ | $\varepsilon > 14.5\%$ | 634 | |

Samples were coated by bar coater on the polyethylene terephthalate (reference) film

A reciprocal relationship was demonstrated between the molar ratio of AA/GMA and the molar substitution of the AA pendant after determining the optimal GMA/MMA molar ratio of 1.6. Correlations between the molar ratio of AA/GMA and the molar substitution of AA pendant were monitored by $^1$H-NMR and hazemeter. The transparency was considerably decreased with an increase of the molar substitution above a level of 93.5% ($A_{1.0}$). The Mandrel bend test and UTM demonstrated the possible application of the copolymer as a protective layer on curved parts. The optimal AA/GMA molar ratio was determined to be 1.4 (molar substitution of 94.3%), which satisfied both the optical and mechanical requirements.

**Acknowledgement** This research was supported by the Ministry of Land, Transportation, and Maritime Affairs (Project No. 08-CTIP-B01), and the Ministry of Knowledge Economy (Project No. 10031999), Republic of Korean.

## References

1. Alemdar N, Karagoz B, Erciyes AT et al (2007) Prog Org Coat 60:69
2. Kardar P, Ebrahimi M, Bastani S et al (2009) Prog Org Coat 64:74
3. Han TL, Kumar R, Rozman H et al (2003) Carbohydr Polym 54:509
4. Hild G, Lamps JP, Rempp P (1993) Polymer 34:2875
5. Bakhshi H, Zohuriaan-Mehr MJ, Bouhendi H et al (2010) J Mater Sci 46:2771. doi:10.1007/s10853-010-5151-7
6. El-Hamouly S, Aziz W, El-Shamy E et al (1992) Polym Degrad Stab 37:41
7. Norakankorn C, Pan Q, Rempel GL et al (2009) Eur Polym J 45:2977
8. Eve S, Mohr J (2010) Appl Surf Sci 256:2927
9. Abusafieh A, Gobran R, Kalidindi SR (1997) J Appl Polym Sci 63:75
10. Jian Z, Yong H, Ming X et al (2009) Prog Org Coat 66:35
11. Hasegawa K, Nishimori H, Tatsumisago M, Minami T (1998) J Mater Sci 33:1095. doi:10.1023/A:1004396703147
12. Ho FFL, Kohler RR, Ward GA (1972) Anal Chem 44:178
13. Fox TG, Flory PJ (1950) J Appl Phys 21:581
14. Montserrat S, Colomer P (1984) Polym Bull 12:173
15. Bakhshi H, Zohuriaan-Mehr M, Bouhendi H et al (2009) Polym Test 28:730
16. Safa KD, Nasirtabrizi MH (2006) Polym Bull 57:293
17. Song P, Zhang Y, Kuang J (2007) J Mater Sci 42:2775. doi:10.1007/s10853-006-1356-1
18. Kalal J, Svec F, Marousek V (1974) J Polymer Sci 47:155
19. Ergozhin E, Bektenov N, Chopabaeva N (2004) Russ J Appl Chem 77:813
20. Nair TM, Kumaran M, Unnikrishnan G et al (2009) J Appl Polym Sci 112:72